ELSEVIER

Surface Science 495 (2001) 68–76

SURFACE SCIENCE

www.elsevier.com/locate/susc

# Morphology of epitaxial metallic layers on MgO substrates: influence of submonolayer carbon contamination

M. Rickart, B.F.P. Roos, T. Mewes, J. Jorzick, S.O. Demokritov *, B. Hillebrands

*Fachbereich Physik and Forschungs- und Entwicklungsschwerpunkt Materialwissenschaften, Universität Kaiserslautern, Erwin-Schrödinger-Strasse 56, D-67663 Kaiserslautern, Germany*

Received 30 May 2001; accepted for publication 6 August 2001

**Abstract**

By investigating the epitaxial growth of Ag(0 0 1) and Au(0 0 1) films and Fe/Ag(0 0 1) and Fe/Au(0 0 1) layered systems on MgO(0 0 1) the influence of carbon contamination of the MgO surface on the morphology of the obtained films is studied. A new technique for the preparation of carbon-free MgO(0 0 1) surfaces using ion beam oxidation is reported. This technique takes advantage of the high chemical activity of dissociated low energy oxygen atoms, which removes the carbon contamination from the MgO surface as confirmed by Auger electron spectroscopy. It is shown that metallic layers grown on carbon-free MgO substrates demonstrate reduced roughness, improved crystallographic quality and enhanced surface magnetic anisotropy compared to those grown on carbon contaminated substrates. 

*Keywords:* Molecular beam epitaxy; Ion bombardment; Surface structure, morphology, roughness, and topography; Carbon; Magnesium oxides; Metal–metal magnetic thin film structures

## 1. Introduction

The generation of atomically flat and chemically clean surfaces is one primary goal of epitaxial thin film growth. It is a well-known fact that the chemical structure and morphology of the substrate surface influences dramatically the quality of the resulting film [1]. Conventionally bulk single crystals of cubic metals (Cu, Ag and Au) with almost atomically flat surfaces are used for a successful epitaxial growth of 3d magnetic Co, Fe, Ni films with a well-layered structure [2,3]. However, for technological applications bulk single crystals are not very suitable as substrates, since they are difficult to manufacture, expensive, and unconvenient in handling. In addition, the use of metallic single crystals impedes resistivity (and magnetoresistivity) measurements on grown films. Therefore, the use of semiconducting or insulating substrates is necessary. Ag and Au buffer films deposited on semiconducting GaAs(0 0 1) are widely used as templates for epitaxial growth of high quality Fe(0 0 1) films and multilayers based on Fe(0 0 1) [4,5]. The buffers serve as barriers for As atoms, which otherwise diffuse from GaAs in Fe and cause a magnetic "dead" layer [6].

* Corresponding author. Tel.: +49-631-205-4075; fax: +49-631-205-4095.

*E-mail address:* demokrit@physik.uni-kl.de (S.O. Demokritov).

0039-6028/01/$ - see front matter 
PII: S0039-6028(01)01504-7

On the other hand insulating MgO is a widely used substrate for growth of metallic films due to its superior high temperature stability and low chemical activity [7,8]. These substrates are comparatively inexpensive and commonly available in a variety of orientations and sample dimensions. MgO has rock-salt structure with a lattice spacing of 0.421 nm. The in-plane mismatch of MgO(0 0 1) to fcc Ag(0 0 1), fcc Al(0 0 1), fcc Au(0 0 1), bcc Fe(0 0 1) and bcc Cr(0 0 1) films is below 4%. However, very often an essential contamination of the MgO surface by carbon is observed [9], prohibiting a good epitaxial growth. Depending on the carbon concentration such a contamination leads to several reconstructions of the deposited films [10]. It is therefore important to understand the influence of the surface structure and its possible contamination on the morphology of high quality thin films grown on these substrates.

In this study we examine the influence of carbon contamination of MgO substrates on the morphology of metallic buffer layers consisting of Ag or Au and the magnetic properties of Fe thin films prepared onto these buffer layers. A new technique for the preparation of carbon-free MgO(0 0 1) surfaces using low energy (<100 eV) oxygen ion beam treatment to remove the carbon contamination on the substrate is presented. We demonstrate that the ion treatment not only results in a removal of carbon from the substrate, but provides a means to smooth the MgO surface.

The surface of commercially available MgO substrates is contaminated mainly by water and carbon. Several methods have been proposed to reduce the carbon contamination and to obtain a carbon free surface of MgO with low roughness: cleavage of the single crystals in ultra high vacuum (UHV) is one of the most practised methods to produce a defect free surface without any contamination [11,12]. Cleaving the substrates in air leaves water at the surface and further contamination and defects even if the substrate is introduced into the UHV immediately. In this case the substrate has to be heated to temperatures up to 600 °C for several hours to remove these adsorbates [13,14]. Another possibility is to cleave the single crystals in air with heating subsequently in oxygen atmosphere at 1000 °C for about 1 h in a high temperature furnace [15,16] in order to reconstruct surface deteriorations arising by storage in air and to diminish the carbon contamination. Chemical cleaning with isopropanol or etching [17] followed by UHV annealing at elevated temperatures [18,19] is also a frequently used method. With these methods it is possible to prepare a smooth single crystal with a vertical surface roughness of 0.2–0.4 nm as corroborated by atomic force microscopy (AFM) [15]. But high temperature treatment of the MgO surface in vacuum and/or in oxygen atmosphere does not result in a carbon-free surface [19], probably, due to continuous diffusion of carbon from the bulk of the crystal to the surface. The ion beam treatment reported here takes place at room temperature, thus avoiding a possible recontamination of the surface by diffusion of carbon from the bulk.

## 2. Experimental procedure and preparation of the substrate surface

MgO(0 0 1) substrates with the nominal purity of 99.9% provided by Crystal GmbH were rinsed in isopropanol at ambient pressure before loading into the UHV. The substrate dimensions are $10 \times 10 \times 0.5$ mm$^3$. All samples were preheated in UHV at a moderate temperature of 150 °C for 30 min to remove water from the surface. Three types of samples were prepared for the experiment: type (A): pre-heated MgO substrates, without any further cleaning before the growth of the metallic layers; type (B): annealed MgO substrates, heated in UHV up to 600 °C for 180 min; type (C): ion beam treated MgO substrates, treated with an atomic oxygen ion beam at room temperature. The oxygen ion beam treatment of the MgO is performed using a novel type of an excited electron cyclotron wave resonance (ECWR) controlled plasma reactor (COPRA 160, CCR Technology). The reactor is a high frequency, low pressure plasma source with an inductive excitation. A crucial advantage of the source is its ability to produce low energy (20–100 eV) ion beams. The ion beam is automatically neutralized by a corresponding electron current, thus minimizing charging effects on the substrate. The filament free design of the source

allows one to perform the ion treatment without contamination of the surface by filament materials. The source produces an oxygen beam with a dissociation degree up to 80%. The ion current density was chosen to be 0.1 mA/cm$^2$ and a process time of 2 min, providing atomic oxygen ion doses of $6 \times 10^{16}$ ions/cm$^2$. Ions with the nominal energy of 35 eV and an energy distribution width below 10% of the nominal energy were used for the ion beam treatment. The ion current density and the ion energy were monitored using a Faraday cup. The pressure in the chamber during the ion beam treatment was $6 \times 10^{-4}$ mbar. A detailed technical description of the source can be found elsewhere [20].

Metallic films were prepared in an UHV multichamber molecular beam epitaxy (MBE) system with a base pressure of less than $5 \times 10^{-11}$ mbar. They were deposited either by a five-pocket electron beam evaporator or a Knudsen cell (Ag) onto the MgO(0 0 1) substrates with deposition rates between 0.01 and 0.1 nm/s as monitored by a quartz microbalance.

Analysis of the surface morphology and the sample structure was performed in situ with low energy electron diffraction (LEED) using a rear view LEED system (ErLEED, VSI GmbH) and reflecting high energy electron diffraction (RHEED, EK-35-R Staib Instruments). For quantative analysis of the diffraction patterns the systems were combined with a CCD camera and a digital image processing system with a resolution of $512 \times 512$ pixels and a dynamic range of 10 bits. The same LEED system was used as a retarding Auger spectrometer to control the carbon contamination. Using Auger spectroscopy it is very difficult to determine the distribution of impurity atoms within the escape depth of the Auger electrons [21]. In this work for quantitative comparison of different Auger spectra the observed intensities of the carbon Auger-peak (KLL line at 275 eV), with the escape depth of the electrons being 3.5 ML, have been recalculated into the effective surface carbon coverage, expressed in percentage of one monolayer [21]. The surface topography in the real space was studied with a commercial Park Scientific Instruments Autoprobe VP 2 UHV device, a combined AFM and scanning tunneling microscope (STM). AFM with a typical lateral resolution of 3 nm was used to for investigations of insulating MgO. Magnetic anisotropies of Fe films were derived from the frequencies of the spin waves determined by means of Brillouin light scattering spectroscopy [22,23].

## 3. Results and discussion

### 3.1. Properties of the MgO substrates

For the type (A) pre-heated MgO substrate an intensive carbon (KLL: 272 eV) peak is found in the Auger electron spectrum as seen in Fig. 1a. The observed intensity of this peak corresponds to an effective carbon coverage of 0.28 ML. A similar amount of carbon impurities is also found on pre-heated substrates, which has not been cleaned with isopropanol. The type (B) annealed substrates reveal a reduced carbon peak, as it is shown in Fig. 1b, with an effective carbon coverage of 0.17 ML. Type (C) substrates cleaned by oxygen ion beam treatment do not demonstrate any carbon contamination above the detection limit of the AES detector, which corresponds to 0.01 ML. During the ion treatment the oxygen ions most likely clean

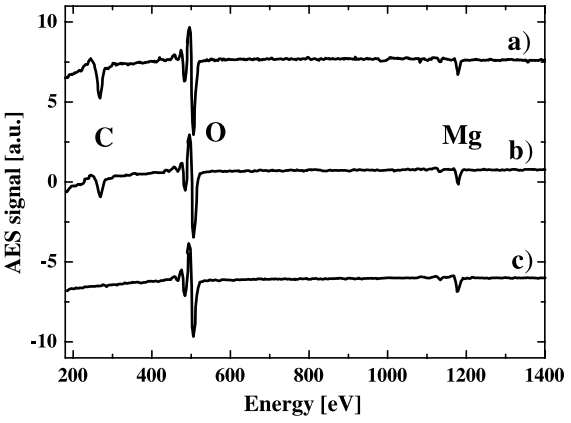


Fig. 1. Auger electron spectra of MgO surfaces. Curve (a) shows a pre-heated substrate, (b) annealed at 600 °C for 3 h and (c) a substrate treated with an oxygen ion beam. No carbon contamination was detected in spectrum (c). All spectra are normalized to the Mg peak for comparison and vertically shifted for clarity.

and "reconstruct" the surface due to the high dissociation degree of the oxygen ions and a chemical reaction with carbon atoms. The obtained $CO_x$ is then pumped out from the UHV chamber. In addition to chemical cleanness the ion beam treated MgO(0 0 1) surfaces exhibit much sharper LEED $(1 \times 1)$ diffraction patterns with essentially no diffuse background compared to the pre-heated or even the annealed sample. The mean coherence length in the electron scattering process is derived from the analysis of the inverse width (FWHM) of the LEED spots multiplied with the corresponding lattice parameter [24]. Since for the case of MgO (and Fe, see below) periodical changes of the spot width as a function of the electron energy have been observed, the obtained mean coherence length, presented in Fig. 2 can be interpreted as a mean terrace width of the surface [24]. As it is seen from Fig. 2, the terrace width is highest for the ion beam treated substrates. AFM topography measurements on the pre-heated substrates showing a rough surface in real space, corroborate the results of our LEED analysis. The measured root mean square (RMS) roughness obtained by AFM on the pre-heated MgO surfaces is 0.7 nm. As seen in Fig. 3 the ion beam treated surface is much smoother showing a measured RMS roughness of about 0.1 nm. Note here, that due to averaging over the finite lateral resolution of the AFM (typically 3 nm), the obtained images may not represent the true surface morphology

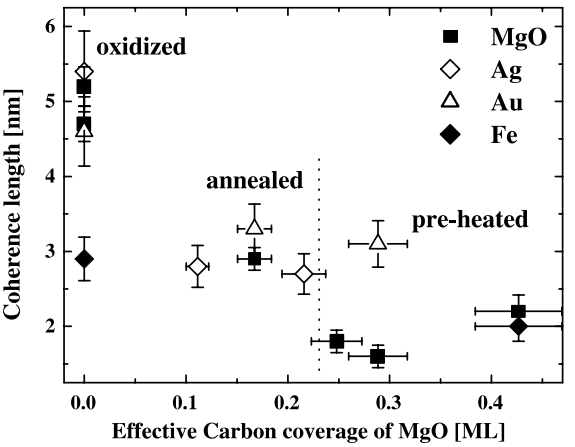


Fig. 2. Mean electron scattering coherence length obtained by evaluation of the LEED spot width of the MgO substrates, the Ag and Au layers and the Fe films for the different preparation methods of independent substrates. The vertical broken line separates regions with different substrate pre-treatment: annealed and pre-heated substrates.

[25]. For the same reason monatomic steps on MgO cannot be resolved. Therefore a direct comparison between the LEED- and the AFM-data is not possible.

### 3.2. Growth of the metallic non-magnetic layers

As it has been already mentioned, MgO with its lattice spacing of 0.421 nm is an excellent substrate for lattice matched growth of fcc Ag(0 0 1) and fcc

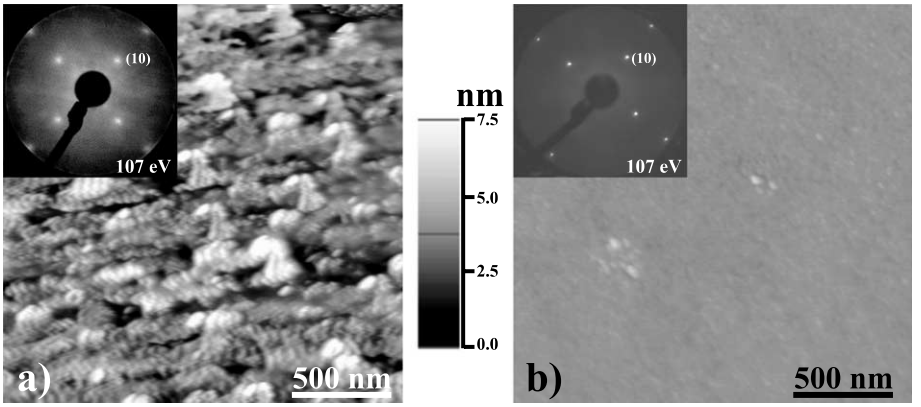


Fig. 3. AFM images of MgO substrates, (a) pre-heated substrate (type A), RMS = 0.7 nm, (b) oxygen ion beam treated substrate (type C), RMS < 0.1 nm. The insets show the corresponding LEED pattern at an energy of 107 eV.

Au(0 0 1) metallic films. Palmberg et al. first reported epitaxial growth of Ag(0 0 1) and Au(0 0 1) on vacuum cleaved MgO(0 0 1) surfaces with a rather high amount of disorder in the films [26]. In agreement with Refs. [26,27] a three-dimensional island growth of Ag and Au on MgO has been observed in the present study, which is due to the high mobility of the Ag and Au atoms on MgO. As layer-by-layer growth is desired an intermediate layer of 1 nm Fe deposited onto the MgO substrate at room temperature improves the growth of the following Ag and Au layers remarkably [28] as one can see in the RHEED images of the Ag films in Fig. 4. The in-plane epitaxial relation between the bcc Fe seed layer and the MgO rock-salt structure is Fe[1 1 0]||MgO[1 0 0] as observed by LEED.

After deposition of the intermediate Fe layer a 150 nm thick Ag layer was deposited at a rate of 0.5 ML/s at a substrate temperature of 120 °C. LEED investigations show that the Ag layer grows with the [1 0 0]-direction parallel to the [1 0 0]-direction of the MgO substrate. STM investigations of the Ag(0 0 1) films prepared on the type (C) substrates reveal atomically smooth terraces with the mean size of 50–70 nm, as seen in Fig. 5. LEED shows an exceptionally intense $(1 \times 1)$ pattern with less background compared to the samples grown on type (A) and (B) substrates, indicating an excellent crystallographic order of the type (C) samples.

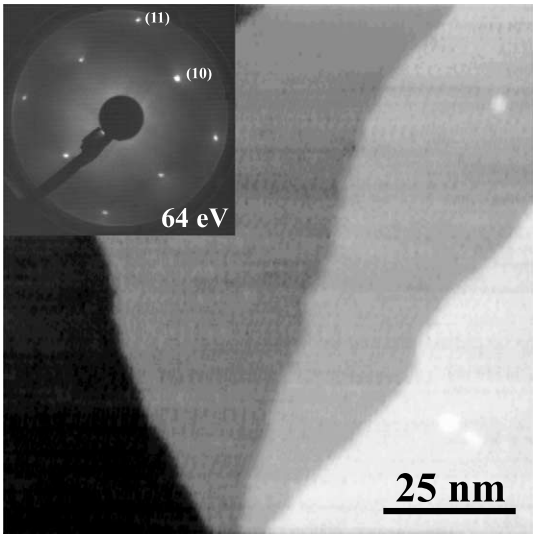


Fig. 5. STM image of an Ag layer demonstrating monatomic steps. The inset shows for Ag a characteristic $(1 \times 1)$ LEED pattern.

Epitaxial Au(0 0 1) films with the thickness of 150 nm were grown on MgO/Fe(0 0 1) at a deposition rate of 0.5 ML/s and a substrate temperature of 120°C. Similar to the growth of Ag the [1 0 0]-direction of Au is orientated along the

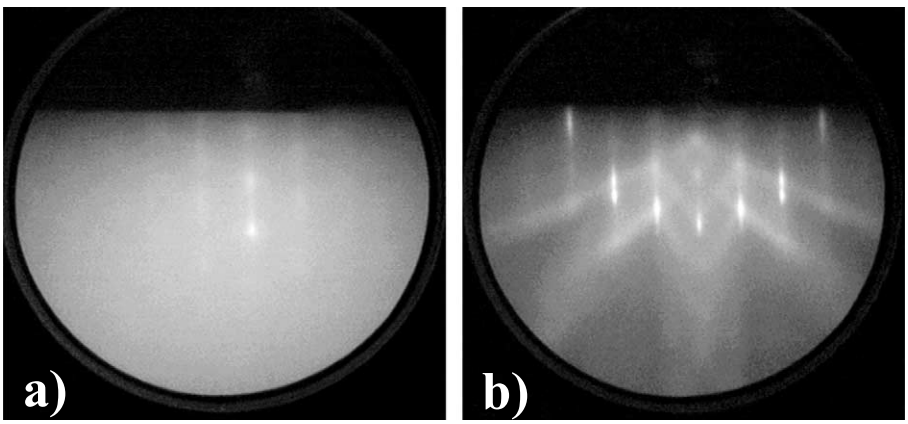


Fig. 4. RHEED images of a 50 nm Ag buffer layer grown onto the MgO substrate (a) without and (b) with a 1 nm Fe intermediate layer. The incident beam with the energy of $E = 15$ keV was directed along the [1 1 0]-direction of the MgO substrate.

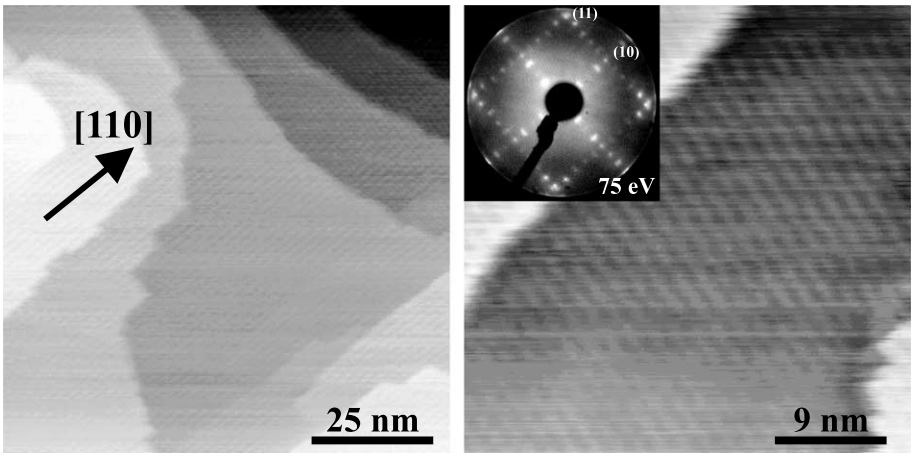


Fig. 6. STM images of an Au layer showing the $(5 \times 20)$ reconstruction and monatomic steps. The inset shows a LEED pattern at 75 eV of the $(5 \times 20)$ reconstruction.

[1 0 0]-direction of MgO. As it is seen from the STM image shown in Fig. 6, Au(0 0 1) grows in a layer-by-layer mode where the uppermost layer forms a $(5 \times 20)$ reconstruction, known from the literature [29]. The atomic rows of the reconstructed surface are orientated parallel the [1 1 0]-directions of Au. The existence of domains with different orientation ([1 1 0] or [1 −1 0]) of the reconstruction restores a fourfold symmetry of the surface, as confirmed by the LEED pattern, shown in the inset of Fig. 6. For a scan area of $0.1 \times 0.1$ μm$^2$ the RMS roughness of the surface is 0.26 nm. The results of the LEED-spot width analysis, presented in Fig. 2 for both Ag and Au films, show that Ag and Au films grown on ion beam treated MgO substrates (type C) exhibit a higher correlation length compared to those grown on annealed substrates (type B) or pre-heated substrates (type A). Note here, that contrary to the case of the MgO surfaces, the spot width of the Ag and Au LEED images do not oscillate as a function of the electron energy. It means, that the observed values of mean coherence length, presented in Fig. 2 for Ag and Au are determined not by atomic steps, but by defects within the atomic layers [24]. This is in agreement with the STM data, which indicate that the mean terrace widths of the Ag and Au surfaces are much larger than the coherence lengths, derived from LEED.

### 3.3. Fe films grown on Ag and Au layers

It is well known that Fe(0 0 1) grows in the bcc phase in a 45° rotation of its lattice on fcc Ag(0 0 1) and Au(0 0 1) with a corresponding in-plane lattice mismatch of less than 1% [4,6]. The high quality of Ag and Au films is an important premise for a good growth of Fe films on those films. In this section we present the results for Fe films deposited on the Ag and Au buffers grown on MgO(0 0 1) surface with different carbon contamination, prepared as it was described above. A 3 nm Fe film was deposited at a temperature of 120 °C and at a rate of 0.04 ML/s. The obtained LEED patterns (Fig. 7a) confirm an epitaxial growth of Fe(0 0 1) films on both Ag and Au buffers. The value of mean coherence lengths derived from the width of the LEED spots for the Fe/buffer/MgO layered system increases from 2 nm for pre-heated substrates to 3 nm, obtained for the systems grown on ion beam treated substrates. No measurable difference between the coherence length for Fe/Ag and Fe/Au systems is observed. The energy dependence of the spot width demonstrates an oscillating behaviour, indicating that the atomic steps of the Fe surface limit the coherence length. This is in agreement with the STM images of Fe shown in Fig. 7 for Fe/Ag and Fe/Au systems. In both cases islands with the mean island

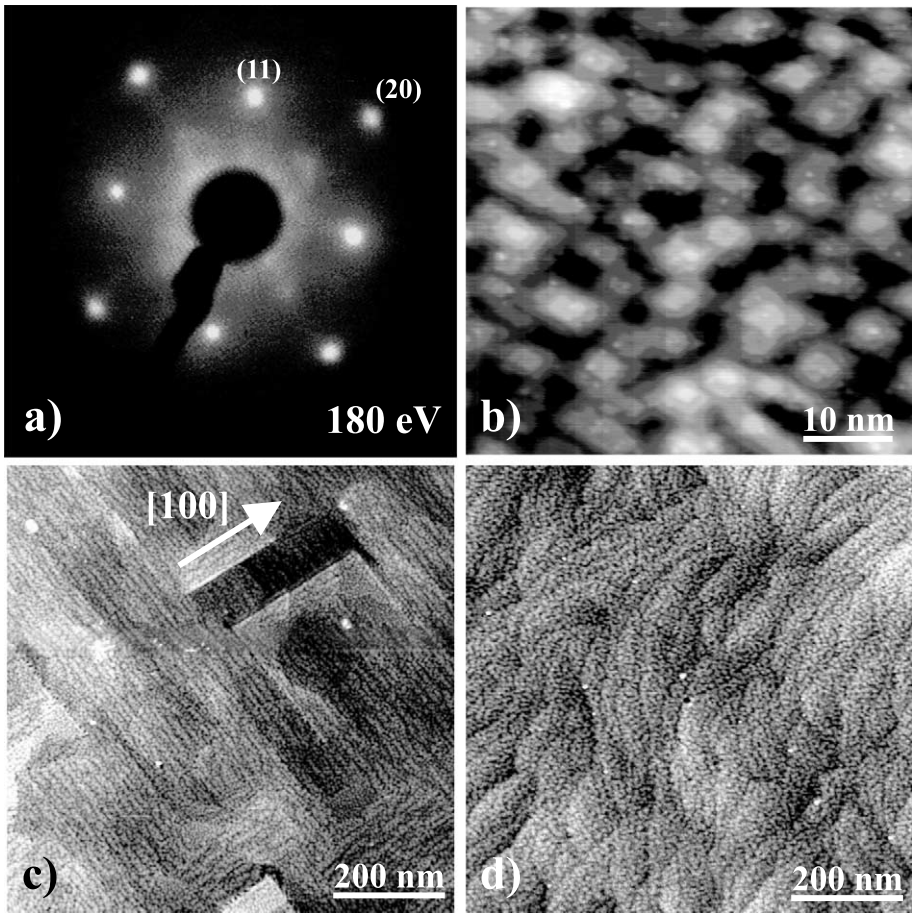


Fig. 7. (a) LEED pattern ($E = 180$ eV) of a 3 nm thick Fe film, epitaxially grown on Au, (b) STM image of the same film showing islands, (c) large scale STM image of the same Fe film, (d) large scale STM image of a 3 nm thick Fe film, epitaxially grown on Ag. Note that in (c) the direction [1 0 0] on Fe corresponds to [1 1 0] on Au.

size of about 15 nm$^2$ and the height of 3–4 ML is observed also in agreement with Ref. [30]. Note, that the large atomically smooth terraces of the buffers can be clearly traced on the Fe surface, as it is seen in Fig. 7c and d.

Surface magnetic anisotropy is a decisive characteristic property of thin magnetic films for application in e.g., magnetic sensors. Magnetic anisotropy in general describes the dependence of the magnetic energy of a sample on the orientation of its magnetization. Contrary to magnetic bulk anisotropies the surface anisotropy describes the contribution of surfaces or interfaces of a film to its magnetic energy. For thin films it can be large enough even to change the equilibrium orientation of the film magnetization [31]. The influence of the morphology of the film on its magnetic anisotropies is thoroughly studied (see e.g. review [3]). Bruno [32] has theoretically shown that surface roughness reduces the surface anisotropy contributions. Thus, Fe films prepared on ion beam treated MgO substrates demonstrate improved smoothness and thus possess an enhanced surface anisotropy with respect to those prepared on the annealed or pre-heated substrates.

The surface magnetic anisotropy of the grown films has been determined ex situ using Brillouin light scattering from spin waves in the film [23].

For ex situ measurements Fe films have been capped with a 4 nm thick Au overlayer in the case of an Au buffer layer and 2 nm Ag and a 2 nm Cr overlayer in the case of an Ag buffer layer to establish chemical symmetry on both interfaces of the Fe films as well as to prevent corrosion. Following the standard approach [3] we characterize the magnetic surface anisotropy by the uniaxial out-of-plane anisotropy constant $k_S^{(2)}$ determined by its contribution to the magnetic energy of the film as $E_V = -2k_S^{(2)} \sin^2\theta/d$, where $E_V$ is density of magnetic energy of the film, $\theta$ is the angle between the film magnetization and the normal to the film plane, and $d$ is the thickness of the film. The surface anisotropy energy changes the frequency of spin waves in the film, which is measured by means of Brillouin light scattering. The details of the measurement set-up and the data evaluation procedure can be found elsewhere [23]. In fact, the measurements reveal a higher value of $k_S^{(2)}$ for the Fe films prepared on the ion beam treated (type (C)) MgO substrates as seen in Fig. 8, which is in agreement with the better quality of the Au and Ag buffer layers described above. The highest value of $k_S^{(2)}$ for the Ag/Fe/Ag system obtained in this study (ion-beam treated substrates) $k_S^{(2)} = 0.6$ erg/cm$^2$ is comparable to the value of $k_S^{(2)} = 0.79$ erg/cm$^2$ obtained on high quality Fe whiskers [33]. The value of $k_S^{(2)} = 0.7$ erg/cm$^2$ obtained in this study for the Au/Fe/Au system is even higher than that one known from the literature ($k_S^{(2)} = 0.54$ erg/cm$^2$) [3,33].

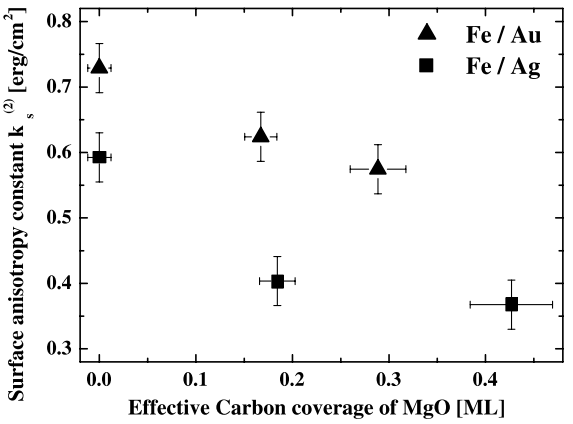


Fig. 8. Evaluation of the uniaxial out-of-plane surface anisotropy constants in dependence of the carbon concentration. Spin wave frequencies were measured by means of Brillouin light scattering spectroscopy and the anisotropy constants calculated.

## 4. Conclusion

We have shown that the growth of Ag(0 0 1) and Au(0 0 1) films on MgO(0 0 1) drastically depends on the carbon contamination of the MgO surface and its smoothness. Using a newly developed technique—low energy ion beam treatment—we succeeded to prepare a carbon free MgO(0 0 1) surface with a very low roughness. We have also presented the layer-by-layer growth of Ag and Au on such carbon free MgO surfaces covered by an intermediate thin Fe layer, as it is confirmed by three independent experimental techniques (LEED, RHEED, and STM). The surface magnetic anisotropies of Fe(0 0 1) films, grown on Ag/Fe/MgO and Au/Fe/MgO-buffers were measured using Brillouin light scattering. The obtained results corroborate a close relationship between high values of the surface anisotropy and high layer quality of the films.

## Acknowledgements

Support by the Deutsche Forschungsgemeinschaft and the ESF programme NANOMAG is gratefully acknowledged. One of the authors (T.M.) acknowledges support by the Studienstiftung des deutschen Volkes.

## References

[1] M.A. Herman, H. Sitter, in: M.B. Panish (Ed.), Molecular Beam Epitaxy, second ed., Springer, Berlin, 1996.
[2] J.A.C. Bland, B. Heinrich (Eds.), Ultrathin Magnetic Structures, vols. I and II, Springer, Berlin, 1994.
[3] U. Gradmann, Magnetism in ultrathin transition metal films, in: K.H.J. Buschow (Ed.), Handbook of Magnetic Materials, vol. 7, North-Holland-Elsevier, Amsterdam, 1993.
[4] P. Grünberg, S. Demokritov, A. Fuss, R. Schreiber, J.A. Wolf, S.T. Purcell, J. Magn. Magn. Mater. 104–107 (1995) 1734.

[5] T. Leeb, M. Brockmann, F. Bensch, S. Miethaner, G. Bayreuther, J. Appl. Phys. 85 (1999) 4964.
[6] J.J. Krebs, B.T. Jonker, G.A. Prinz, J. Appl. Phys. 61 (1987) 2596.
[7] Y.C. Lee, P. Tong, P.A. Montano, Surf. Sci. 181 (1987) 559.
[8] C. Li, R. Wu, A.J. Freeman, C.L. Fu, Phys. Rev. B 48 (1993) 8317.
[9] F. Didier, J. Jupille, Surf. Sci. 307–309 (1994) 587.
[10] G. Gewinner, J.C. Peruchetti, A. Jaegle, R. Riedinger, Phys. Rev. Lett. 43 (1979) 935.
[11] J.B. Zhou, H.C. Lu, T. Gustafsson, P. Häberle, Surf. Sci. 302 (1994) 350.
[12] G. Fahsold, A. Priebe, N. Magg, A. Pucci, Thin Solid Films 364 (2000) 177.
[13] C. Duriez, C. Chapon, C.R. Henry, J.M. Rickard, Surf. Sci. 230 (1990) 123.
[14] T. Suzuki, R. Souda, Surf. Sci. 445 (2000) 506.
[15] F. Klinkhammer, Ch. Sauer, E.Yu. Tsymbal, S. Handschuh, Q. Leng, W. Zinn, J. Magn. Magn. Mater. 161 (1996) 49.
[16] L.W. Guo, T. Hanada, H.J. Ko, Y.F. Chen, H. Makino, T. Yao, Surf. Sci. 445 (2000) 151.
[17] S.S. Perry, H.I. Kim, S. Imaduddin, S.M. Lee, P.B. Merril, J. Vac. Sci. Technol A 16 (6) (1998) 3402.
[18] J. Dekoster, S. De Groote, T. Kobayashi, G. Langouche, J. Magn. Magn. Mater. 148 (1995) 93.
[19] S.M. Jordan, J.F. Lawler, R. Schad, H. van Kempen, J. Appl. Phys. 84 (1998) 1499.
[20] M. Weiler, K. Lang, E. Li, J. Robertson, Appl. Phys. Lett. 72 (1998) 1314.
[21] M.P. Seah, in: D. Briggs, M.P. Seah (Eds.), Practical Surface Analysis, Wiley, New York, 1983, p. 181.
[22] S. Demokritov, E. Tsymbal, J. Phys, Cond. Mat. 6 (1994) 7145.
[23] B. Hillebrands, Brillouin light scattering from layered magnetic structures, Topics Appl. Phys. 75 (2000) 174.
[24] M. Henzler, Appl. Surf. Sci. 11/12 (1982) 450.
[25] H.N. Yang, G.C. Wang, T.M. Lu, Diffraction from Rough Surfaces and Dynamic Growth Fronts, World Scientific, Singapore, 1993.
[26] P.W. Palmberg, T.N. Rhodin, C.J. Todd, Appl. Phys. Lett. 11 (1967) 33.
[27] T. Suzuki, S. Hishita, K. Oyoshis, R. Souda, Surf. Sci. 442 (1999) 291.
[28] P. Etienne, J. Massies, S. Lequien, R. Cabanel, F. Petroff, J. Crystal Growth 111 (1991) 1003.
[29] M.A. van Hove, R.J. Koestner, P.C. Stair, J.P. Biberian, L.L. Kesmodel, I. Bartos, G.A. Somorjai, Surf. Sci. 103 (1981) 189.
[30] D.E. Bürgler, C.M. Schmidt, J.A. Wolf, T.M. Schaub, H.-J. Güntherodt, Surf. Sci. 366 (1996) 295.
[31] M.L. Neel, J. Phys. Rad. 15 (1954) 376.
[32] P. Bruno, J. Phys. F: Met. Phys. 18 (1988) 1291.
[33] B. Heinrich, Z. Celinski, J.F. Cochran, A.S. Arrott, K. Myrtle, J. Appl. Phys. 70 (1991) 5769.